Numerical Example

As a specific example, a foamed-in-plane polyurethane cylinder is considered. The core and skin are both assumed to be isotropic and linearly elastic, with the same properties in tension and compression. Using E_c = 22,000 psi, ν_c = $\frac{1}{3}$, E = 42,000 psi, ν = $\frac{1}{3}$, h = 0.15 in., L = 1.00 in., and R = 0.488 in., the results obtained are as shown in Table 1.

References

[1] Bert, C. W. and Hyler, W. S., "Design Considerations in Material Selection for Rocket-Motor Cases," *Journal of Spacecraft and Rockets*, Vol. 4, No. 6, June 1967, pp. 705–715.

[2] Kujawa, F. M., "High Density Urethane Foam Prepared by the One-Shot Technique," *Journal of Cellular Plastics*, Vol. 1, No. 3, July 1965, pp. 400–405.

[3] Reissner, E., "Memorandum on Effect of Soft Solid Core on Buckling of Axially Loaded Circular Cylindrical Shells," Structures Study 64, Aug. 12, 1957, Lockheed Aircraft Corp., Missile Systems Div., Sunnyvale, Calif.

[4] Zak, A. R. and Bollard, R. J. H., "Elastic Buckling of Cylindrical Thin Shells Filled with an Elastic Core," *ARS Journal*, Vol. 32, No. 4, April 1962, pp. 588–593.

[5] Seide, P., "The Stability Under Axial Compression and Lateral Pressure of Circular-Cylindrical Shells with a Soft Elastic Core," *Journal of the Aerospace Sciences*, Vol. 29, No. 7, July 1962, pp. 851–862.

[6] Yao, J. C., "Buckling of an Axially Compressed Long Cylindrical Shell with an Elastic Core," *Transactions of the ASME, Ser. E: Journal of Applied Mechanics*, Vol. 29, No. 2, June 1962, pp. 329–334.

[7] Lu, S. Y. and Nash, W. A., "Buckling of Thin Cylindrical Shells Stiffened by a Soft Elastic Core," *Simplified Calculation Methods of Shell Structures*, edited by A. Paduart and R. Duton, North-Holland Publishing Co., Amsterdam, Holland, 1962, pp. 475–481.

[8] Almroth, B. O. and Brush, D. O., "Postbuckling Behavior of Pressure-or Core-Stabilized Cylinders under Axial Compression," *AIAA Journal*, Vol. 1, No. 10, Oct. 1963, pp. 2338–2341.

[9] Lemke, D. G., "Buckling of a Composite Orthotropic Cylinder Containing an Elastic Foundation," AIAA Paper 63-233, Los Angeles, Calif. 1963.

[10] Holston, A., Jr., "Stability of Inhomogeneous Anisotropic Cylindrical Shells Containing Elastic Cores," *AIAA Journal*, Vol. 5, No. 6, June 1967, pp. 1135–1138.

[11] Tarnopol'skii, Yu. M. and Roze, A. V., "Distortion of Cross Sections During Deformation of Oriented Glass-Reinforced Plastics," *Polymer Mechanics*, Vol. 1, No. 5, Sept.-Oct. 1965, pp. 69–75.

[12] Myint-U. T., "Stability of Axially Compressed Core-Filled Cylinders," *AIAA Journal*, Vol. 4, No. 3, March 1966, pp. 552–553.

[13] Timoshenko, S. P., "On the Correction for Shear of the Differential Equation for Transverse Vibrations of Prismatic Bars," *Philosophical Magazine*, Ser. 6, Vol. 41, 1921, pp. 742–746.

[14] Reissner, E., "The Effect of Transverse Shear Deformation on the Bending of Elastic Plates," *Transactions of the ASME, Ser. E: Journal of Applied Mechanics*, Vol. 12, No. 1, March 1945, pp. A69–A77.

[15] Love, A. E. H., *A Treatise on the Mathematical Theory of Elasticity*, 4th ed., Dover, New York, 1944, Chap. 24.

[16] Sanders, J. L., Jr., "An Improved First Approximation Theory for Thin Shells," TR R-24, 1959, NASA.

[17] Reissner, E., "Small Bending and Stretching of Sandwich-Type Shells," TN 1832, 1949, NACA (superseded by Rept. 975, 1950, NACA).

[18] Tasi, J., "Effect of Heterogeneity on the Stability of Composite Cylindrical Shells under Axial Compression," *AIAA Journal*, Vol. 4, No. 6, June 1966, pp. 1058–1062.

[19] Freudenthal, A. M., "Deformation and Failure Analysis of Reinforced Grains," *Mechanics and Chemistry of Solid Propellants*, edited by A. C. Eringen et al., Pergamon Press, Oxford, 1967, pp. 463–483.

[20] Benning, C. J., "Polyethylene Foam III—Orientation in Thermoplastic Foams," *Journal of Cellular Plastics*, Vol. 3, No. 4, April 1967, pp. 174–184.

[21] Guz', A. N., "The Accuracy of the Kirchhoff-Love Hypothesis in Determining Critical Forces in the Theory of Elastic Stability," *Soviet Physics—Doklady*, Vol. 13, No. 3, Sept. 1968, pp. 270–271.

Electron Energy Distributions in an Ion Engine Discharge

ANTHONY R. MARTIN*
The City University, London, England

THE presence of a high-energy, primary electron component in the discharge plasma of mercury electron-bombardment ion engines is well known.[1–4] These primaries, arising from electrons which are accelerated into the plasma through the cathode sheath, have also been found in the present tests in the discharges of laboratory models of ion engines using argon as the working gas. This Note presents the results of energy distribution analyses carried out on the probe curves obtained in such an engine.

Energy Distribution Analysis

The Langmuir probe curves obtained in this type of discharge have the general shape shown in the uncorrected curve of Fig. 1 when plotted semilogarithmically. They are usually analyzed by assuming that the energy distribution of the electrons collected by the probe is composed of a high-energy, monoenergetic component superimposed upon a low-energy, Maxwellian component. This assumption enables the two components to be separated and values for electron densities and energies can then be obtained from the curves. The methods of Strickfaden and Geiler[1] and Knauer et al.[3] lead to slightly different values of the primary electron energy; here the latter method has been employed in analyzing the linear curves, and produces corrected plots of the form shown in Fig. 1. The validity of this method of analysis can be checked by determining the energy distributions found in practice. The usually quoted way of doing this is the Druyvesteyn method,[5,6] which involves taking second derivatives of the probe curve. If this method is carried out graphically, it is inaccurate and tedious.

Medicus[7,8] has developed a simple, quick, accurate graphical method, which has been used here to determine the experimental energy distributions given by Langmuir probe

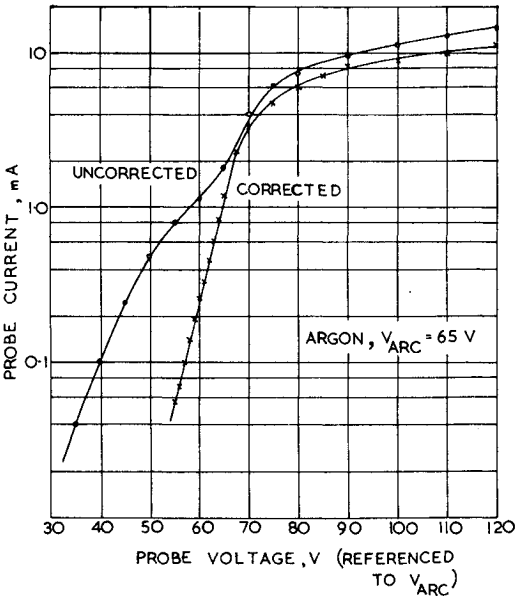

Fig. 1 Corrected and uncorrected semilogarithmic probe curves for argon.

Received October 28, 1970. The author was in receipt of a Science Research Council maintenance grant during the period of this work.

* Graduate Student, Department of Aeronautics.

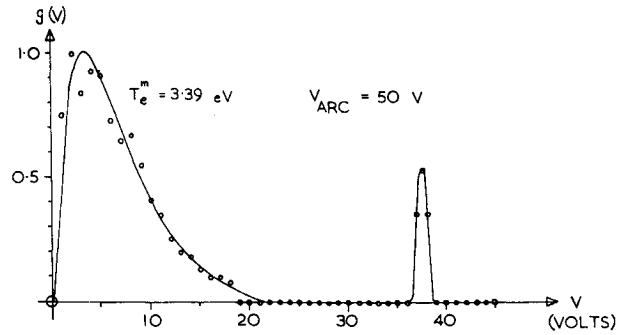

Fig. 2 Electron distribution in the discharge at V_{ARC} = 50 v.

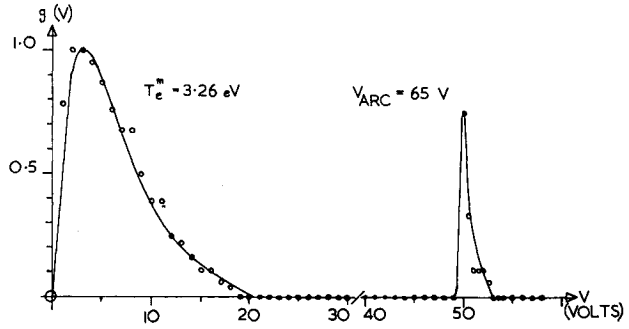

Fig. 3 Electron distribution at V_{ARC} = 65 v.

curves in argon. The method is based on the fact that the current to a small probe is produced by electrons with kinetic energies equal to or greater than the electron-retarding probe potential. It simply involves subdividing the voltage axis into increments ΔV of equal size and constructing the tangents to the probe curve at the midpoints of these increments. This will give increments Δi on the current axis. It can be shown[7] that the energy distribution $g(V)$ at any point is then given by

$$g(V) = (4/n_e)(m_e/2e)^{1/2}V^{-1/2}(\Delta i/\Delta V)$$

where n_e is the total electron number density and V is the voltage of the probe at each point where the tangent is drawn, i.e., the midpoint of each increment ΔV. If the electron current to the probe rises linearly with voltage (as in the case of the collection of monoenergetic electrons) then clearly Δi will be zero for each ΔV, and hence $g(V)$ will be zero. If the current increases or decreases more strongly than a linear relationship, however, then Δi is nonzero and $g(V)$ is greater than zero.

Experimental Results

The measurements were made in a laboratory model of an ion engine using commercially pure, dried argon as a working gas. The engine was of the Kaufman type, and the discharge chamber used was 10 cm in diameter and 20 cm long. A heated axial tungsten filament was used. At the flow rates employed the pressure in the chamber was between 10^{-4} and 10^{-3} torr during discharge operation. An axial magnetic field of flux density 30 gauss at the center of the chamber was used. The Langmuir probes were made from pure, cleaned tungsten wire with a cylindrical collecting area 11 mm long and 0.5 mm in diameter.

Figure 2 shows the electron energy distribution in a discharge plasma at an arc voltage V_{ARC} of 50 v. Three separate evaluations of the probe curve were made and averaged to reduce graphical errors arising from the inaccuracy in drawing the tangents. The curves were traced, at several different current sensitivities, by an X-Y plotter onto 38- × 25-cm graph paper. Values of $g(V)$ are presented as proportional to $V^{-1/2}\Delta i/\Delta V$ and are normalized to 1.0 arbitrary unit at the maximum. The solid line drawn through the low-energy groups is the Maxwellian distribution for the electron temperature, T_e^m = 3.39 ev, obtained from a semilogarithmic plot corrected in the manner described by Knauer et al.[2,3] While there is a fair amount of scatter in the data points, the experimental $g(V)$ values follow this Maxwellian very well. The high-energy, primary group of electrons can be clearly seen, with a mean energy E_e^P corresponding to 37.5 ev. The value of E_e^P obtained from the linear curve in this case was 39.0 ev, which is in reasonable agreement. The full width at half maximum ($FWHM$) of the primary peak is 1.40 ev.

Table 1 Probe curve analysis results

V_{ARC} (V)	T_e^m (ev)	E_e^P(ev) Linear curve	E_e^P(ev) $g(V)$ curve	$FWHM$ (ev)
50	3.39	39.0	37.5	1.40
55	3.69	39.5	41.0	1.75
60	3.69	45.0	46.0	1.50
65	3.26	54.0	50.0	0.90
70	3.35	57.5	57.0	0.65
75	3.04	63.0	63.0	0.75
80	3.04	71.5	73.0	0.90

Figure 3 shows the distribution for V_{ARC} = 65 V, and is the analysis of the curve plotted in Fig. 1. Figure 4 shows the distribution for V_{ARC} = 80 V. These curves are again the averages of three evaluations, normalized to 1.0 arbitrary unit. In both cases the solid line drawn through the low-energy group is the Maxwellian corresponding to the temperature determined from corrected semilogarithmic plots.

Some relevant results obtained from a series of probe curves in the range V_{ARC} = 50–80 V are presented in Table 1.

From Table 1 and Figs. 2–4, several observations can be made for an argon plasma:

a) The low-energy and high-energy groups of electrons are distinct and separate, with no observable spread of energies between them.

b) The low-energy group has a distribution which closely corresponds to the Maxwellian drawn for the temperature obtained from corrected semilogarithmic plots.

c) The primary electron energy obtained from linear curves corresponds well with the mean energy obtained from energy distribution curves.

d) The $FWHM$ of the primary peaks is always less than 2 ev, and sometimes as low as 0.65 ev; i.e., the peaks are sharp and distinct.

Hence, we may conclude that the assumption of a monoenergetic group of primary electrons in the argon discharge plasma is valid to a good approximation, and that the method of analysing the uncorrected linear Langmuir probe curves, as described by Knauer et al.,[3] will give accurate and meaningful results.

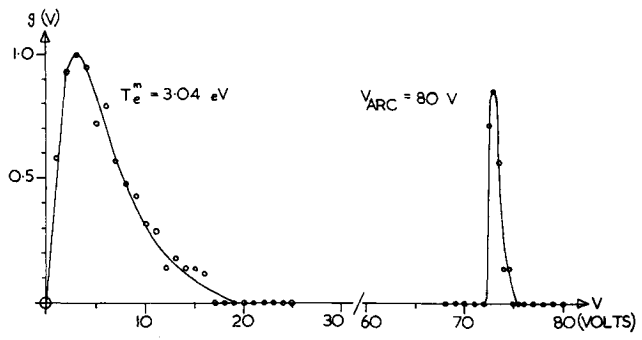

Fig. 4 Electron distribution at V_{ARC} = 80 v.

References

[1] Strickfaden, W. B. and Geiler, K. L., "Probe Measurements of the Discharge in an Operating Electron Bombardment Engine," *AIAA Journal*, Vol. 1, No. 8, Aug. 1963, pp. 1815–1823.

[2] Knauer, W. and Poeschel, R. L., "Semi-annual Report—Discharge Chamber Studies for Mercury Bombardment Ion Thrusters," CR-72350, 1967, NASA.

[3] Knauer, W. et al., "Final Report—Discharge Chamber Studies for Mercury Bombardment Ion Thrusters," CR-72440, Sept. 1968, NASA.

[4] Masek, T. D., "Plasma Characteristics of the Electron Bombardment Ion Engine," TR 32-1271, April 1968, Jet Propulsion Lab., Pasadena, Calif.

[5] Mott-Smith, H. M. and Langmuir, I., "The Theory of Collectors in Gaseous Discharges," *Physical Review*, Vol. 28, Oct. 1926, pp. 727–763.

[6] Druyvesteyn, M., "Der Niedervoltbogen," *Zeitschrift für Physik*, Vol. 64, 1930, pp. 781–798.

[7] Medicus, G., "Simple Way to Obtain the Velocity Distribution of the Electrons in Gas Discharge Plasmas from Probe Curves," *Journal of Applied Physics*, Vol. 27, No. 10, Oct. 1956, pp. 1242–1248.

[8] Medicus, G., "Diffusion and Elastic Collision Losses of the 'Fast Electrons' in Plasmas," *Journal of Applied Physics*, Vol. 29, No. 6, June 1958, pp. 903–908.

Calculation of Relaxing Turbulent Boundary Layers Downstream of Tangential Slot Injection

DENNIS M. BUSHNELL*

NASA Langley Research Center, Hampton, Va.

Nomenclature

C_f = skin-friction coefficient
l = mixing length
M_∞ = freestream Mach number
q = heating rate
s = slot height
S_t = Stanton number
T = temperature
t = slot lip thickness
U = longitudinal velocity
x,y = cartesian coordinates along and normal to the surface
$y_{s,1}$ = distance to inner boundary of mixing region
$y_{s,2}$ = distance to outer boundary of mixing region
y_c = slot half height
ψ = mixing angle (Fig. 1)
δ = total viscous layer thickness
λ = ratio of average specific mass flow in slot to value at edge of boundary layer

Subscripts

e = local external to boundary
max = maximum value
0 = reference value
t = isentropic stagnation conditions
w = wall

CURRENT interest exists in the possibility of using tangential slot injection for reducing heat transfer and skin friction on hypersonic vehicles.[1] Several low-speed experimental investigations of the downstream effects of tangential injection have been conducted which could provide information for the assessment of such a cooling system (see Ref. 2 for a partial list of these investigations). An accurate prediction method has been developed for the far field ($x/s > 30$) effects of tangential injection, primarily for the low-speed case.[3] Data also exist for tangential slot injection at supersonic and hypersonic speeds (Refs. 4, 5, and 6, for example). The present Note describes the application of a simple calculation method for compressible relaxing slot flows. Agreement with the data indicates that the simplified approach described here applies to the near slot ($x/s < 30$) as well as the far slot ($x/s > 30$) regions of the flow. This approach could be used, for example, in parametric studies to estimate the effects on the relaxation process of slot-to-edge total temperature ratio, slot height to boundary-layer height, and slot Mach number. The present method uses the turbulent boundary-layer computational procedure of Ref. 7 with the conservation equations for the mean flow solved by an implicit finite difference procedure and a turbulent Prandtl number relating the eddy viscosity and eddy conductivity. The solutions presented herein use a static turbulent Prandtl number[7] of 0.9. Note that the present method applies only to the matched static pressure case where the exit pressure of the slot flow essentially equals the value in the external flow, i.e., where mixing dominates the problem.

Before the method of Ref. 7 can be applied to relaxing tangential slot flows, appropriate modifications must be made to the mixing length model for eddy viscosity. Figure 1 illustrates the method employed here to model the mixing length for tangential slot flows. We assume the slot flow mixes with the initial boundary-layer flow in a region whose growth can be characterized to first order by a mixing angle ψ (Fig. 1a). This assumption allows computation of the nominal thickness of an effective mixing region as a function of distance downstream from the slot. With this model final results were fairly insensitive to the value of ψ assumed. On a test case to be considered in this Note, for example, increasing the ψ value from 4° to 6° decreased the cooling length (where T_{aw} first becomes larger than the slot flow total temperature) by 10%. Unpublished work by Beckwith and Bushnell at Langley Research Center indicates that the computation of the mixing of a trace species inserted in the initial boundary layer can be used to determine the mixing

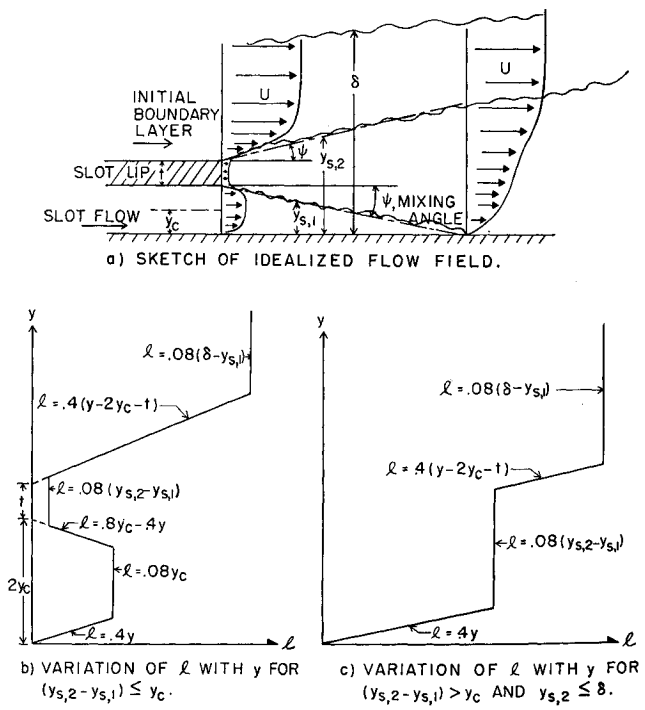

Fig. 1 Assumed mixing length distributions.

Received October 30, 1970.

* Head, Flow Analysis Section, Aero-Physics Division.